

# Design of Low Noise Micro Liter Syringe Pump for Quartz Crystal Microbalance Sensor

Ridha N. Ikhsani  
*Department of Physics*  
*Brawijaya University*  
 Malang, Indonesia  
 ridha.fisika@gmail.com

D.J. Djoko H. Santjojo  
*Department of Physics*  
*Brawijaya University*  
 Malang, Indonesia  
 dsantjojo@ub.ac.id

Setyawan P. Sakti  
*Department of Physics*  
*Brawijaya University*  
 Malang, Indonesia  
 sakti@ub.ac.id\*

**Abstract**—An injection pump was a critical aspect in the used of Quartz Crystal Microbalance (QCM) biosensor or chemical sensor in liquid. It is required that the pump should have variable speed and doesn't introduce pressure noise to the QCM sensor. In this work, the pump was developed using a micro stepper motor with a microliter syringe. The mechanical transmission transforms the rotational displacement of the motor into a translational displacement of the syringe. The flow rate of the injection pump could affect the signal pattern indicated by a signal spike or instability of the sensor resonance frequency. The developed system successfully minimized the spike signal and improved the stability of the sensor resonance by the used of the microliter syringe pump with optimizing the reaction chamber of the QCM sensor. The flow rate of the pump can be controlled with a minimum speed of 0.7  $\mu\text{L}/\text{second}$  for water. At low flow rate, there was a negligible or none of the spike signal observed during the injection and ejection of the liquid. However, at a high flow rate, few signal spikes may be observed.

**Keywords**—*Microliter syringe pump, stepper motor, QCM, flow rate.*

## I. INTRODUCTION

As one of the ultra mass-sensitive sensor, the Quartz Crystal Microbalance (QCM) sensor have been used in many applications such as for biosensors applications [1], [2]. The response of frequency change from the QCM sensor caused by a mass change on top of the sensor surface. The QCM as a biosensor works in a liquid environment [3]–[6]. In this experiment, one of the sensor surfaces is put in contact with buffer or sample solution. The buffer and sample solution covered the whole side of the sensor surface. On the other hand, the other side of the sensor surface is in contact with the air.

For sensor preconditioning, immobilization or reaction, buffer or sample solution was injected into the sensor surface. There are two methods for injecting the buffer or sample solution of target molecules on top of the sensor. A flow injection method [7] or the liquid drop method [8]. Although these methods are suitable for injection the buffer or sample solution, both methods have significant shortcomings.

The flow injection system required a complex handling system, and also a short pressure change at the sensor surface. The injection method with a microliter syringe pump has been reported in previous work [9], the injection speed also affected the resonance frequency of the sensor. The small spike signal or noise was detected. Optimizing the injection method is needed to minimize the existence of the spike and to simplify the handling system. On the other hand,

the liquid drop method suffered from a compressional wave or disturbance to the sensor [10]. Usually, a significant change in the sensor resonance frequency was observed at the time of liquid drop.

In the present study, we developed a controllable and low noise microliter syringe pump which can be used to fill the QCM sensor surface in the adjacent reaction cell. The pump was designed for injecting and ejecting the buffer or sample solution with a few disturbance on the frequency responses by minimizing the hydrostatic pressure changes. The microliter syringe pump system was developed and controlled by using a microcontroller. A simple user interface was designed to control the movement of the microliter syringe pump. The used of software to control the system minimized the complexity of the electronics circuit and also providing connectivity with the acquisition software for further development. In addition, the new design of cell reaction chamber is utilized to minimize the spike signal of the frequency response. The speed of a micro stepper motor, which meant the injection or ejection flow rate, was varied during the experiment to investigate the effect of flow rate.

## II. SYSTEM DESIGN AND METHOD

### A. Hardware and software design

In this experiment, the system of microliter pump was developed using a microliter syringe. The syringe stroke was controlled using a 42BYGH-48 stepper motor linear actuator, with a mechanical transmission system. The motor speed and direction were controlled by using a PIC18F45K50 microcontroller. The stepper motor driver DRV8255 was used to drive a motor stepper with PWM micro stepping. The communication between the computer software and the pump system was done using the USB interface. A USB CDC protocol was used for the communication between the microliter pump device and the computer.

The command from the computer was sent to the microcontroller in the pump system using a defined data format and translated by the microcontroller to control the system. The integrated pump system consists of a mechanical part for microliter syringe pump, oscillator circuit subsystem which can be connected directly to the cell reaction with QCM Sensor inside of the chamber, directions control subsystem, frequency counter subsystem, and frequency capture program. The block diagram of a measurement system for QCM sensor including a microliter pump is illustrated in Fig.1.

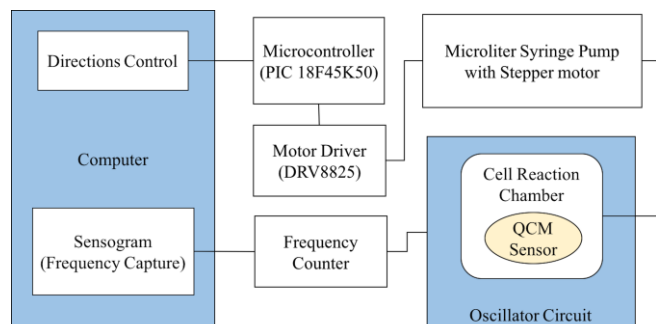


Fig. 1. Block diagram of the measurement system for the QCM sensor.

A disposable syringe with a maximum volume of 100  $\mu\text{L}$  was used as a pump. The syringe has a stroke length of 85 mm. The maximum stroke length of the microliter syringe pump system is 60 mm in parallel with a maximum volume of 75  $\mu\text{L}$ . The mechanical transmission transforms the rotational displacement of the motor into a translational displacement of the syringe. The maximum distance of the displacement transducer was set according to the syringe length. An emergency stop was placed to stop the displacement transducer movement to protect the syringe stroke movement. The design of the microliter pump with a micro-stepper motor and a syringe is presented in Fig. 2.

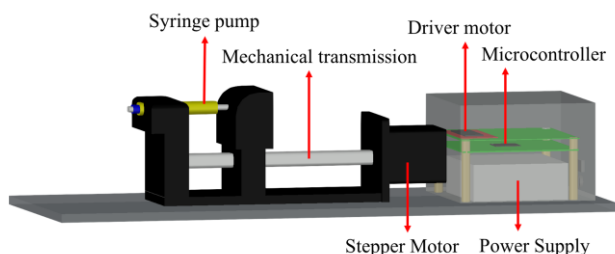


Fig. 2. Design of microliter injection pump.

The PIC 18F45K50 and other electronic part and the system power supply was packed and integrated into the mechanical translator unit. It is placed directly behind the motor stepper unit and spared the space in another end for the reaction cell installation.

The reaction cell made from PMMA (Poly Methyl Methacrylate) and PLA (Poly Lactic Acid). The central part of this reaction cell is a reaction chamber on top of the sensor surface. The liquid inlet and outlet in the edge of the chamber were connected to the tilted injection channel. The position of the inlet and outlet channel was placed far from the center of the sensor disc. The reaction cell is depicted in Fig. 3.

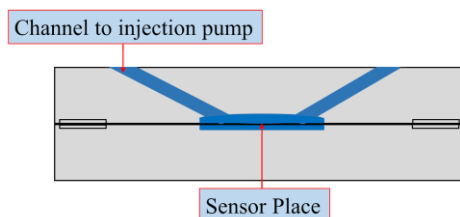


Fig. 3. Design of cell reaction in the experiment (front view).

The sensor was mounted inside of the cell reaction. A silicon ring was used as a damper and spacer to minimize mechanical stress during installation in the cell reaction and sealed the liquid in the reaction chamber.

A simple user interface was developed to control the syringe pump. The interface is depicted in Fig. 4. The software primarily comprised of directions and flow rate control. The user sets the flow rate of the pump by inputting the value of the desired liquid volume per minute in  $\mu\text{L}$ . The minimum value of the volume to be injected 10  $\mu\text{L}$ , and the maximum volume is 75  $\mu\text{L}$ .

The movement of the pump was started when the user presses the direction button (REVERSE button or FORWARD button). Rapid filling and disposal of the reaction chamber were facilitated by FILL UP SYRINGE and FULL DISPENSED buttons.

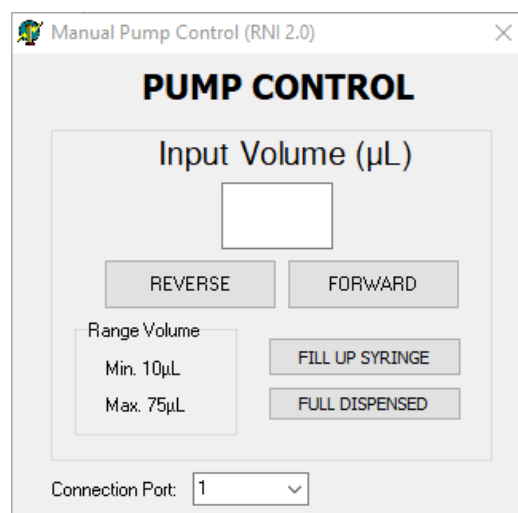


Fig. 4. The user interface of the microliter syringe pump system.

### B. Microliter Pump Calibration

The developed injection system using the syringe pump was calibrated using the volumetric method. Calibration was done using a digital balance with a resolution of 2 mg. The volume was converted from the measured water mass based on the water density at room temperature.

The calibration was done by varying the motor speed. The mass of the ejected water from the syringe pump was weighted using the balance. The amount of the water was determined by the motor speed and time. The ejected water was weighted using the balance and then converted as volume. The results of the volume calibration process are shown in Fig. 5, and Fig. 6.

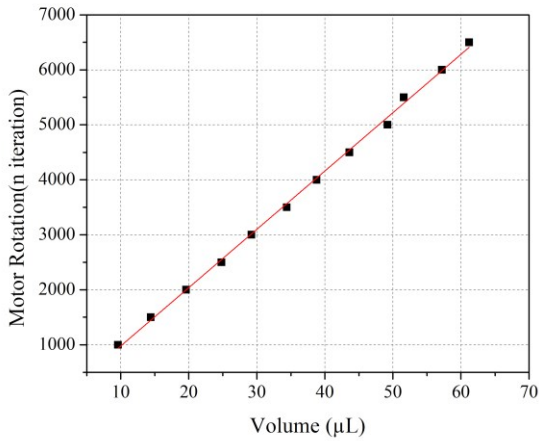


Fig. 5. Volume calibration for injection speed at a 6.3  $\mu\text{L}$  per second.

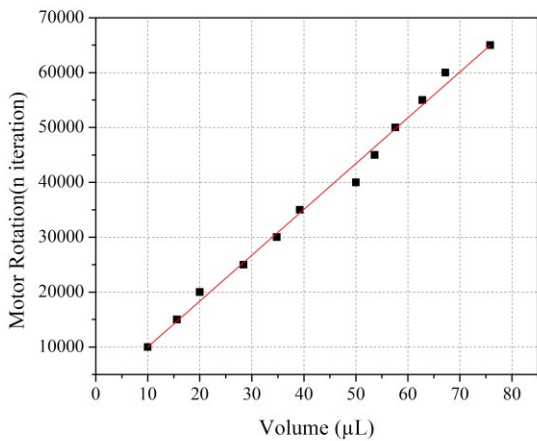


Fig. 6. Volume calibration for injection speed at a 0.7  $\mu\text{L}$  per second.

### C. Experimental System Setup

The complete setup of the system for the experiment was presented in Fig. 7. It consists of the designed injection pump, the reaction cell, and a frequency counter. The outlet of the syringe pump was connected to the reaction cell to the inlet port by using a silicone hose and a needle.

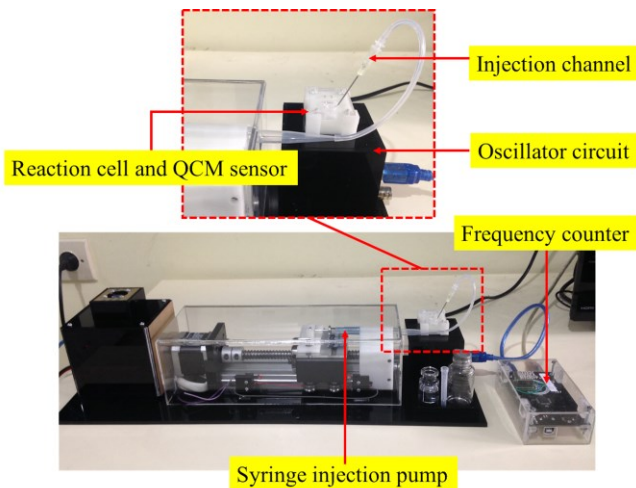


Fig. 7. Photograph of the system

Under the reaction cell, there was an oscillator which able to drive the sensor in contact with air as well as in contact with water. The oscillator was connected to the frequency counter.

### III. RESULT AND DISCUSSION

The pump effect to the sensor was measured by varying the water flow rate injected and ejected into and from the reaction chamber. Initially, the reaction chamber was filled with water to bring the state of the sensor into a condition of one sensor surface in contact with water. After the new resonance frequency in contact with water was reached, the sequence of injection and or ejection was done.

The resonance frequency of the sensor was recorded during the injection and ejection process. The frequency resolution of the frequency counter was 1 Hz. Therefore, any change of the resonance frequency of the sensor equal to or higher than 1 Hz can be measured. Frequency measurement was done every second.

After a stable resonance frequency when the sensor in the reaction cell was observed, a 30  $\mu\text{L}$  water was injected into the reaction chamber to cover the sensor surface with water. The sensor surface gradually contacts with water in parallel with the injected water. The transition of the surface contact of the sensor from entirely in contact with air and totally in contact with water affect the sensor resonance frequency. The resonance frequency of the sensor was rapidly decreased as the resonance frequency of the sensor change according to the Kanazawa-Gordon equation [11]. After the sensor surface was fully covered with water, a new resonance frequency of the sensor was reached. The new resonance frequency was indicated by a constant value of the recorded frequency. Fig. 8 shows the frequency transition of the sensor in contact with air and in contact with water.

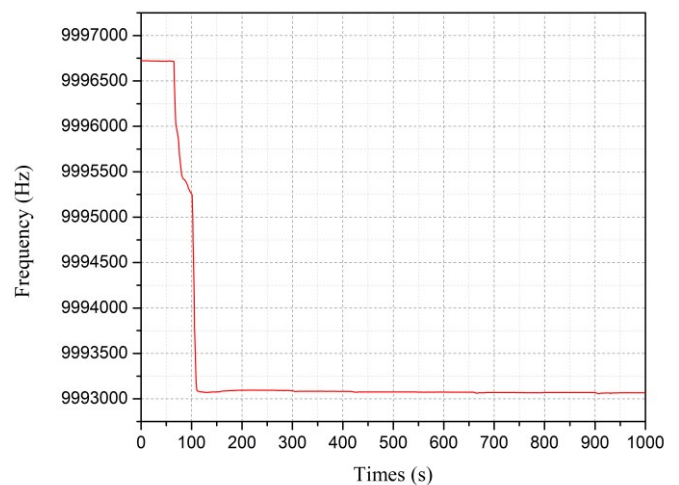


Fig. 8. Sensor resonance frequency during the transition from contacting with air and water

After the resonance frequency was steady, an amount of 10  $\mu\text{L}$  water was injected into the reaction cell. This injection pushes the water to flow into the reaction chamber. The excess water went out onto the outlet. The change in the water flow caused a small pressure change on the sensor surface which affect the resonance frequency of the sensor.

Fig. 9. and Fig. 10. shows the response frequency of the sensor during the injection and ejection process.

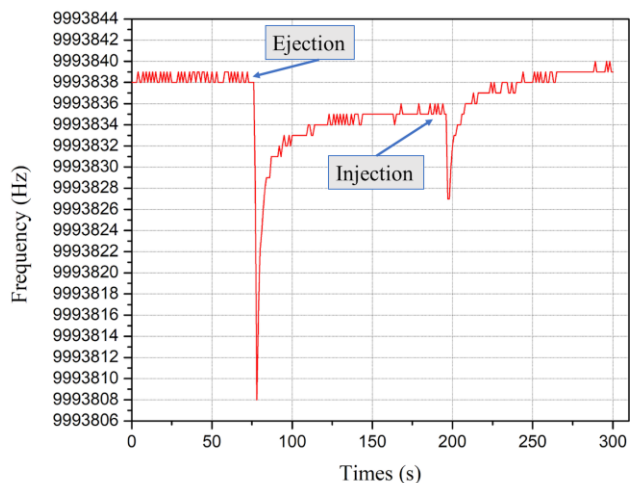


Fig. 9. Sensor resonance frequency caused by 10  $\mu\text{L}$  water injection and ejection at a speed of 6.3  $\mu\text{L}$  per second.

At the event of water injection, the frequency counter recorded a change of the resonance frequency of the sensor. The frequency of the sensor was abruptly decreased, and followed by a gradual increase of the sensor resonance frequency back to the initial frequency.

The similar response was observed during the reverse direction of water flow. When the water was ejected out, the resonance frequency of the sensor changed in a short time resulted in a small spike and then followed by a returning resonance frequency to the initial frequency.

Fig. 9. shows the resonance frequency of the sensor during injection and ejection of 10  $\mu\text{L}$  water at a speed of 6.3  $\mu\text{L}$  per second. During the injection and ejection process, there is no frequency spike, or noise detected. It means that the pressure change caused by injection and ejection speed of 6.3  $\mu\text{L}$  per second does not affect to emersions of frequency spike or noise. However, we found a decreasing frequency change during the injection and ejection process. A short frequency change was observed about 20-30 Hz during the first ejection sequence of 10  $\mu\text{L}$  water. After the ejection process was stopped, the resonance frequency reverts to the initial frequency with 2 Hz different. In the injection process, the short frequency change was observed around 10 Hz. After the injection was stopped, the resonance frequency was changed to the first initial frequency with the same value.

The same response is also observed during the injection and ejection process of 10  $\mu\text{L}$  water at a speed of 0.7  $\mu\text{L}$  per second. During the injection and ejection process, the short frequency change was also observed. The resonance frequency decreases during its process. However, after the injection and ejection process, the resonance frequency reverts to the initial frequency with the same value, as shown in the Fig. 10.

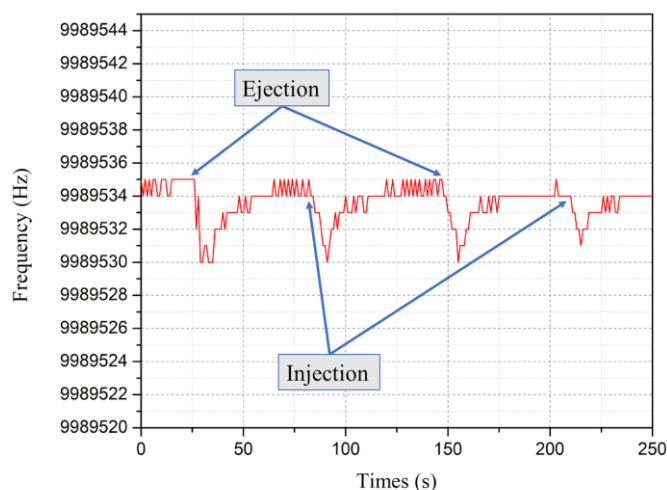


Fig. 10. Sensor resonance frequency caused by 10  $\mu\text{L}$  water injection and ejection at a speed of 0.7  $\mu\text{L}$  per second.

The resonance frequency change of the sensor, during water ejection at the flow rate of 6.3  $\mu\text{L}$  per second was higher than the resonance frequency change caused by the injection of 0.7  $\mu\text{L}$  per second. At 6.3  $\mu\text{L}$  per second, the frequency change caused by ejection was 30 Hz, on the other hand, the frequency change was 5 Hz at an ejection speed of 0.7  $\mu\text{L}$  per second. Meanwhile, the resonance frequency change from the sensor during water injection was also slightly higher at speed 6.3  $\mu\text{L}$  per second, than the water injection speed of 0.7  $\mu\text{L}$  per second. The frequency change was only 4-5 Hz at an injection speed of 0.7  $\mu\text{L}$  per second. At the 6.3  $\mu\text{L}$  per second, the frequency change during water injection was 7 Hz. The higher flow rate theoretically resulted in a pressure change on the sensor surface. The change in pressure on the sensor surface nor other liquid property change during the water flow resulted in a frequency change of the sensor. This result was similar to the other works about resonance frequency effect of syringe pump [9], and a relationship between gas pressure and a frequency sensor [12]. The stability of the sensor resonance in contact with liquid is better compared to work done with a 35MHz QCM sensor [13] and comparable with the work done using 9MHz QCM sensor [14].

The experiment shows that a higher flow rate resulted in a bigger frequency spike during injection and ejection. Therefore, it is necessary to control the flow rate to minimize the frequency spike. During the use of the sensor system for biomolecule reaction, it should be noticed that the frequency change in within 100 seconds after the injection and ejection should consider the effect of the liquid flow on the sensor surface. To minimize the effect one should consider using a slowest liquid flow rate.

#### IV. CONCLUSION

The microliter pump using a syringe injection was successfully developed and its flow rate effect to the QCM sensor was examined. The microliter pump system was able to inject or eject a liquid to the sensor system with a flow rate of 0.7 and 6.3  $\mu\text{L}$  per second. Both water injection and ejection slightly affected the resonance frequency of the sensor. Higher flow rate resulted in a higher frequency change caused by a short pressure change. The flow rate of less than 0.7  $\mu\text{L}$  per second affects to the resonance

frequency of the sensor by 5 Hz at a water ejection and 4-5 Hz at water injection.

#### ACKNOWLEDGMENT

The authors would like to express their gratitude to Collaborative Research Center for Advanced System and Material Technology (CRC-ASMAT) and Sensor Technology Laboratory, for their help during the experiment of this work. This work was part of a research project funded by the Ministry of Research, Technology and Higher Education of the Republic of Indonesia under the HIKOM research grant scheme.

#### REFERENCES

- [1] S. Kurosawa, J.-W. Park, H. Aizawa, S.-I. Wakida, H. Tao, and K. Ishihara, "Quartz crystal microbalance immunosensors for environmental monitoring," *Biosens. Bioelectron.*, vol. 22, no. 4, pp. 473–481, Oct. 2006.
- [2] P. F. Höök and M. Rudh, "Quartz crystal microbalances ( QCM ) in biomacromolecular recognition," *bisensor*, no. March, 2005.
- [3] K. Zhang *et al.*, "A microfluidic system with surface modified piezoelectric sensor for trapping and detection of cancer cells," *Biosens. Bioelectron.*, vol. 26, no. 2, pp. 935–939, Oct. 2010.
- [4] R. L. Caygill, G. E. Blair, and P. a Millner, "A review on viral biosensors to detect human pathogens," *Anal. Chim. Acta*, vol. 681, no. 1–2, pp. 8–15, Nov. 2010.
- [5] J. W. Thies, P. Kuhn, B. Thürmann, S. Dübel, and A. Dietzel, "Microfluidic quartz-crystal-microbalance (QCM) sensors with specialized immunoassays for extended measurement range and improved reusability," *Microelectron. Eng.*, vol. 179, pp. 25–30, 2017.
- [6] Z. A. Talib, Z. Baba, Z. Kurosawa, H. A. A. Sidek, A. Kassim, and W. M. M. Yunus, "Frequency Behavior of a Quartz Crystal Microbalance (QCM) in Contact with Selected Solutions," *Am. J. Appl. Sci.*, vol. 3, no. 5, pp. 1853–1858, 2006.
- [7] M. Michalzik, R. Wilke, and S. Büttgenbach, "Miniaturized QCM-based flow system for immunosensor application in liquid," *Sensors Actuators B Chem.*, vol. 111–112, no. SUPPL., pp. 410–415, Nov. 2005.
- [8] S. P. Sakti, N. Chabibah, S. P. Ayu, M. C. Padaga, and A. Aulanni'am, "Development of QCM Biosensor with Specific Cow Milk Protein Antibody for Candidate Milk Adulteration Detection," *J. Sensors*, vol. 2016, pp. 1–7, 2016.
- [9] R. N. Ikhsani and S. P. Sakti, "Flow rate effect of syringe pump on quartz crystal microbalance sensor resonance frequency stability," in *Proceeding - 2016 International Seminar on Sensors, Instrumentation, Measurement and Metrology, ISSIMM 2016*, 2017.
- [10] R. Lucklum, S. Schranz, C. Behling, F. Eichelbaum, and P. Hauptmann, "Analysis of compressional-wave influence on thickness-shear-mode resonators in liquids," *Sensors Actuators A Phys.*, vol. 60, no. 1–3, pp. 40–48, May 1997.
- [11] K. Keiji Kanazawa and J. G. Gordon, "The oscillation frequency of a quartz resonator in contact with liquid," *Anal. Chim. Acta*, vol. 175, pp. 99–105, 1985.
- [12] A. Wessels, B. Kl?ckner, C. Siering, and S. R. Waldvogel, "Practical strategies for stable operation of HFF-QCM in continuous air flow.," *Sensors*, vol. 13, no. 9, pp. 12012–12029, 2013.
- [13] J. Liang, J. Zhang, W. Zhou, and T. Ueda, "Development of a Flow Injection Based High Frequency Dual Channel Quartz Crystal Microbalance," *Sensors*, vol. 17, no. 5, p. 1136, 2017.
- [14] L. Rodriguez-Pardo, A. M. Cao-Paz, and J. Fariña, "Design and characterization of an active bridge oscillator as a QCM sensor for the measurement of liquid properties and mass films in damping media," *Sensors Actuators, A Phys.*, vol. 276, pp. 144–154, 2018.